Lawrence Berkeley National Laboratory

Title
Detecting Light Dark Matter with Magnons

Permalink
https://escholarship.org/uc/item/1993n3hq

Authors
Trickle, Tanner
Zhang, Zhengkang
Zurek, Kathryn M

Peer reviewed

Detecting Light Dark Matter with Magnons

Tanner Trickle[1,2,3] Zhengkang Zhang[3,1,2] and Kathryn M. Zurek[3,2,1]

[1]*Department of Physics, University of California, Berkeley, California 94720, USA*
[2]*Theoretical Physics Group, Lawrence Berkeley National Laboratory, Berkeley, California 94720, USA*
[3]*Walter Burke Institute for Theoretical Physics, California Institute of Technology, Pasadena, California 91125, USA*

Scattering of light dark matter with sub-eV energy deposition can be detected with collective excitations in condensed matter systems. When dark matter has spin-independent couplings to atoms or ions, it has been shown to efficiently excite phonons. Here we show that, if dark matter couples to the electron spin, magnon excitations in materials with magnetic dipole order offer a promising detection path. We derive general formulae for single magnon excitation rates from dark matter scattering, and demonstrate as a proof of principle the projected reach of a yttrium iron garnet target for several dark matter models with spin-dependent interactions. This highlights the complementarity of various collective excitations in probing different dark matter interactions.

Introduction.—Direct detection of dark matter (DM) has undergone a dramatic expansion of scope in recent years. Well-motivated theories where sub-GeV DM arises in a hidden sector or hidden valley, with new weakly or strongly coupled dynamics (see, e.g., Refs. [1–8] for early examples), have given impetus to new ideas to search for light DM. Conventional nuclear recoils, well-matched kinematically to search for weak-scale DM, are not effective for light DM—once the DM mass drops below the target nucleus mass, the fraction of the DM's kinetic energy that can be deposited on the target falls. Beyond nuclear recoils, better DM-target kinematic matching allows us to probe qualitatively new parameter space, through lighter targets (e.g., electrons) with ∼eV (as in semiconductors and atoms [9–18] as well as molecules [19–21]) or ∼meV (as in superconductors [22–24] and Dirac materials [25]) energy gaps. Reading out such small energy depositions is achieved through improvements to cryogenic superconducting calorimeters, such as transition edge sensors (TES) and microwave kinetic inductance devices (MKIDs). *Collective* excitations, such as phonons in superfluid helium [26–29] and crystals [30,31], open new avenues for good kinematic matching. For example, the presence of $\mathcal{O}(10\text{–}100)$-meV gapped optical phonons in some systems facilitates the extraction of a large fraction of DM's kinetic energy for DM as light as ∼10 keV.

Beyond kinematics, there is also a *dynamics* aspect of the problem—depending on how the DM couples to standard model (SM) particles, different target responses are relevant. A familiar example from nuclear recoils is the presence of several nuclear responses—spin-independent (SI), spin-dependent (SD), etc.—which can probe different DM-SM interactions [32–35]. Together they provide broad coverage of the DM theory space, with various target nuclei offering complementary information. Another example is dark photon mediated DM: a material with a strong optical response, such as a superconductor, has weak reach since the effective coupling of the dark photon is suppressed due to in-medium effects, while Dirac materials and polar crystals, which have weaker optical response, have excellent reach [25,30,31]. Similarly, collective excitations can arise from different degrees of freedom, such as charge or spin, and some excitations may be advantageous over others for certain types of DM couplings. Therefore, in order to identify the broadest DM detection strategy, it is important to consider collective excitations of all types.

From this perspective, previous proposals via phonon excitations are aimed at probing SI responses. While they cover many simple DM models, including those with a dark photon or scalar mediator, there are other scenarios that are equally plausible, where the leading DM-SM interactions lead to stronger SD responses. For example, in dark photon mediated models, the DM may in fact be charge neutral, but couple to the dark photon via a higher multipole, e.g., magnetic dipole or anapole [33,35–45]. Also, a spin-0 mediator may dominantly couple to the pseudoscalar (rather than scalar) current of SM fermions. In these scenarios, summarized in Table I, SI responses are suppressed compared to the previously considered cases, and ideas of detecting SD responses are needed. More

generally, SI and SD couplings can coexist, so it is desirable to pursue detection channels for both in order to have a more complete picture of DM interactions.

In this Letter, we propose a novel detection path for spin-dependent light DM-electron interactions via magnon excitations. Magnons are quanta of collective spin wave excitations in condensed matter systems that exhibit magnetic dipole order in the ground state. They can be thought of as the SD counterpart of phonons for DM detection with similar kinematics. We demonstrate as a proof of principle that single magnon excitations can probe interesting DM scenarios through scattering, thus broadening the coverage of the DM theory space. In future work we will pursue DM (in particular axion DM) absorption through magnon excitations.

Magnons in magnetically ordered materials.—Magnetic order can arise in solid state systems due to the interplay between electron-electron interactions, electron kinetic energy and Pauli exclusion (see, e.g., Refs. [46,47]). Such systems are usually described by a spin lattice model, e.g., the Heisenberg model,

$$H = \frac{1}{2} \sum_{l,l'=1}^{N} \sum_{j,j'=1}^{n} J_{ll'jj'} S_{lj} \cdot S_{l'j'}. \quad (1)$$

Here l, l' label the magnetic unit cells, and j, j' label the magnetic atoms or ions inside the unit cell. Depending on the sign of the exchange coupling $J_{ll'jj'}$, the spins S_{lj} and $S_{l'j'}$ tend to align or antialign. The low energy excitations are obtained by applying the Holstein-Primakoff transformation to expand the spins around the ordered ground state in terms of bosonic creation and annihilation operators $\hat{a}^\dagger$, $\hat{a}$. The quadratic part of the Hamiltonian can then be diagonalized via a Bogoliubov transformation (see the Supplemental Material [48] for details),

$$\begin{pmatrix} \hat{a}_{j,k} \\ \hat{a}_{j,-k}^\dagger \end{pmatrix} = \begin{pmatrix} U_{j\nu,k} & V_{j\nu,k} \\ V_{j\nu,-k}^* & U_{j\nu,-k}^* \end{pmatrix} \begin{pmatrix} \hat{b}_{\nu,k} \\ \hat{b}_{\nu,-k}^\dagger \end{pmatrix}, \quad (2)$$

$$H = \sum_{\nu=1}^{n} \sum_{k \in 1\text{BZ}} \omega_{\nu,k} \hat{b}_{\nu,k}^\dagger \hat{b}_{\nu,k}, \quad (3)$$

so that $\hat{b}^\dagger$, $\hat{b}$ are creation and annihilation operators of the canonical magnon modes, which are collective excitations of the spins. For a system with N magnetic unit cells and n magnetic atoms/ions in the unit cell, there are n magnon branches, labeled by ν, with N modes on each branch, labeled by momentum vectors k within the first (magnetic) Brillouin zone (1BZ). The $n \times n$ matrices U, V can be calculated for each k.

Magnon excitation from dark matter scattering.—If the DM couples to the electron spin, it can scatter off the target material and create magnon excitations [49]. Suppose the nonrelativistic effective Lagrangian takes the form

$$\mathcal{L} = -\sum_{\alpha=1}^{3} \hat{\mathcal{O}}_\chi^\alpha(q) \hat{S}_e^\alpha, \quad (4)$$

where α denotes the Cartesian coordinates, and q is the momentum transfer from the DM to the target. The operators $\hat{\mathcal{O}}_\chi$ that follow from the three Lagrangians we consider are listed in Table I. Focusing on transitions from the ground state to single magnon states $|\nu, k\rangle$, we obtain the matrix element as (see the Supplemental Material [48] for details)

$$\mathcal{M}_{\nu,k}^{s_i s_f}(q) = \delta_{q,k+G} \frac{1}{\sqrt{N\Omega}} \sum_{\alpha=1}^{3} \langle s_f | \hat{\mathcal{O}}_\chi^\alpha(q) | s_i \rangle \epsilon_{\nu,k,G}^\alpha, \quad (5)$$

where Ω is the volume of the magnetic unit cell, G denotes a reciprocal lattice vector, and $|s_{i,f}\rangle$ are the initial and final DM spin states. $\epsilon_{\nu,k,G}$ is the analog of polarization vectors for the magnon modes,

$$\epsilon_{\nu,k,G} = \sum_{j=1}^{n} \sqrt{\frac{S_j}{2}} (V_{j\nu,-k} r_j^* + U_{j\nu,k}^* r_j) e^{iG \cdot x_j}, \quad (6)$$

where $r_j^\alpha \equiv R_j^{\alpha 1} + i R_j^{\alpha 2}$ parameterize the spin orientations in the ground state,

$$S_{lj}^\alpha = \sum_\beta R_j^{\alpha\beta} S_{lj}'^\beta, \quad \{\langle S_{lj}'^1 \rangle, \langle S_{lj}'^2 \rangle, \langle S_{lj}'^3 \rangle\} = \{0, 0, S_j\}, \quad (7)$$

TABLE I. Dark matter models, having Lagrangian $\mathcal{L}$, with SD interactions considered in this work; these models are particularly well motivated when DM does not carry a charge of any type, see, e.g., Refs. [33,35–45]. χ is a spin-1/2 DM particle, and V, ϕ are ultralight (typically $\ll$ eV) spin-1, spin-0 mediators, respectively. g_χ, g_e are dimensionless couplings, and Λ_χ is the effective theory cutoff. In the nonrelativistic limit, these Lagrangians reduce to the operators $\hat{\mathcal{O}}_\chi^\alpha$ (with Cartesian coordinates $\alpha = 1, 2, 3$), as in Eq. (4). $q \equiv |q|$ is the momentum transfer, and $\hat{S}_\chi^\alpha = \sigma^\alpha/2$ is the DM spin operator. $\bar{\sigma}_e$ is the reference cross section defined in Eq. (11) that we will use to present the reach.

Model	$\mathcal{L}$	$\hat{\mathcal{O}}_\chi^\alpha$	$\bar{\sigma}_e$
Magnetic dipole DM	$\mathcal{L} = (g_\chi/\Lambda_\chi)\bar{\chi}\sigma^{\mu\nu}\chi V_{\mu\nu} + g_e \bar{e}\gamma^\mu e V_\mu$	$\hat{\mathcal{O}}_\chi^\alpha = (4g_\chi g_e/\Lambda_\chi m_e)[\delta^{\alpha\beta} - (q^\alpha q^\beta/q^2)]\hat{S}_\chi^\beta$	$\bar{\sigma}_e = (g_\chi^2 g_e^2/\pi)\{[6m_\chi^2 + m_e^2]/[\Lambda_\chi^2(m_\chi + m_e)^2]\}$
Anapole DM	$\mathcal{L} = (g_\chi/\Lambda_\chi^2)\bar{\chi}\gamma^\mu\gamma^5\chi\partial^\nu V_{\mu\nu} + g_e\bar{e}\gamma^\mu e V_\mu$	$\hat{\mathcal{O}}_\chi^\alpha = (2g_\chi g_e/\Lambda_\chi^2 m_e)\epsilon^{\alpha\beta\gamma} iq^\beta \hat{S}_\chi^\gamma$	$\bar{\sigma}_e = (g_\chi^2 g_e^2/\pi)(3\alpha^2\mu_{\chi e}^2/2\Lambda_\chi^4)$
Pseudomediated DM	$\mathcal{L} = g_\chi\bar{\chi}\chi\phi + g_e\bar{e}i\gamma^5 e\phi$	$\hat{\mathcal{O}}_\chi^\alpha = -(g_\chi g_e/q^2 m_e)iq^\alpha \mathbb{1}_\chi$	$\bar{\sigma}_e = (g_\chi^2 g_e^2/4\pi)(\mu_{\chi e}^2/\alpha^2 m_e^4)$

and $\boldsymbol{x}_j \equiv \boldsymbol{x}_{lj} - \boldsymbol{x}_l$ is the position of the jth site within a magnetic unit cell. As a simple example, a ferromagnet with one magnetic ion per unit cell ($n = 1$) has $\boldsymbol{r} = (1, i, 0)$, $U = 1$, $V = 0$, and thus, $\boldsymbol{\epsilon} = \sqrt{S/2}(1, i, 0)$ for all $\boldsymbol{k}$ and $\boldsymbol{G}$, reminiscent of a photon polarization vector.

From Eq. (5) we see that for given $\boldsymbol{q}$, only the magnon modes with $\boldsymbol{k} \in 1\text{BZ}$ satisfying $\boldsymbol{q} = \boldsymbol{k} + \boldsymbol{G}$ for some $\boldsymbol{G}$ can be excited, due to lattice momentum conservation. Summing over s_f and averaging over s_i, we obtain

$$\overline{|\mathcal{M}_{\nu,\boldsymbol{k}}(\boldsymbol{q})|^2} = \frac{\delta_{\boldsymbol{q},\boldsymbol{k}+\boldsymbol{G}}}{N\Omega^2} \text{tr}(\hat{\rho}_\chi \hat{\mathcal{O}}_\chi^\alpha(\boldsymbol{q}) \hat{\mathcal{O}}_\chi^{\dagger\beta}(\boldsymbol{q})) \epsilon_{\nu,\boldsymbol{k},\boldsymbol{G}}^\alpha \epsilon_{\nu,\boldsymbol{k},\boldsymbol{G}}^{*\beta}, \quad (8)$$

where $\hat{\rho}_\chi = [1/(2S_\chi + 1)]\mathbb{1}_{2S_\chi+1}$ is the density matrix for the spin of the incoming DM. The total event rate per unit target mass is then obtained as

$$R = \frac{1}{\rho_T} \frac{\rho_\chi}{m_\chi} \int d^3 v_\chi f(\boldsymbol{v}_\chi) \sum_\nu \sum_{\boldsymbol{k} \in 1\text{BZ}} \Gamma_{\nu,\boldsymbol{k}}(\boldsymbol{v}_\chi), \quad (9)$$

$$\Gamma_{\nu,\boldsymbol{k}}(\boldsymbol{v}_\chi) = 2\pi \sum_{\boldsymbol{q}=\boldsymbol{k}+\boldsymbol{G}} \overline{|\mathcal{M}_{\nu,\boldsymbol{k}}(\boldsymbol{q})|^2} \delta(E_{\chi_i} - E_{\chi_f} - \omega_{\nu,\boldsymbol{k}}), \quad (10)$$

where ρ_T is the target mass density, $\rho_\chi = 0.3$ GeV/cm^3 is the local DM energy density, $E_{\chi_i} = \frac{1}{2} m_\chi v_\chi^2$, $E_{\chi_f} = (m_\chi \boldsymbol{v}_\chi - \boldsymbol{q})^2/(2m_\chi)$. We assume the DM velocity distribution $f(\boldsymbol{v}_\chi)$ is Maxwell-Boltzmann, with dispersion 220 km/s, truncated by the galactic escape velocity 500 km/s, and boosted to the target rest frame by the Earth's velocity in the galactic rest frame, 240 km/s. We take the continuum limit $\sum_{\boldsymbol{k} \in 1\text{BZ}} \to N\Omega \int [d^3 k/(2\pi)^3]$, where R becomes N independent.

Projected reach.—As a first demonstration of the detection concept, we consider a yttrium iron garnet (YIG, $Y_3Fe_5O_{12}$) target. YIG is a classic ferrimagnetic material that has been extensively studied and well characterized, and can be readily synthesized with high quality [50,51]. It has been exploited for axion DM detection via absorption in an external magnetic field [52–54]. Here we focus on DM scattering for which external fields are not necessary for producing a signal. Particular detection schemes will be explored in future work.

YIG has 20 magnetic ions Fe^{3+} per unit cell, with effective spins $S_j = 5/2$ ($j = 1, \ldots, 20$) coming from five $3d$ electrons with quenched orbital angular momentum. The ground state has the 12 tetrahedral-site and 8 octahedral-site spins pointing in opposite directions. Taking the crystal parameters from Ref. [55] and Heisenberg model parameters from Ref. [50], we diagonalize the magnon Hamiltonian using the algorithm of Ref. [56] to obtain the magnon spectrum $\omega_{\nu,\boldsymbol{k}}$ and the U, V matrices that enter the rate formulae. For simplicity, we fix the direction of the DM wind to be parallel (perpendicular) to the ground state spins for the magnetic dipole and anapole (pseudomediated)

models, which maximizes the event rate. For fixed target orientation, we find a daily modulation of $\mathcal{O}(10\%)$, which could be utilized for distinguishing DM signals from backgrounds. Following common practice, we present the projected reach in terms of a reference cross section $\bar{\sigma}_e$ defined from DM-free electron scattering. Here we generalize the definition in Ref. [9] beyond SI interactions by defining

$$\bar{\sigma}_e \equiv \frac{\mu_{\chi e}^2}{16\pi m_\chi^2 m_e^2} \overline{|\mathcal{M}_{\text{free}}|^2}(q = \alpha m_e, v^\perp = \alpha), \quad (11)$$

where $\mu_{\chi e}$ is the DM-electron reduced mass, $\alpha = 1/137$ is the fine structure constant, and $v^\perp$ is the component of the relative velocity perpendicular to $\boldsymbol{q}$. The reference cross section for each model is given in Table I.

Our results are shown in Fig. 1 for m_χ up to 10 MeV, assuming 3 events on a YIG target (colored solid curves) with kilogram-year exposure and, following convention for easy comparison to other experiments, no background [57]. Beyond 10 MeV, the simple Heisenberg model description breaks down in part of the kinematic integration region where q exceeds the inverse ionic radius of Fe^{3+}; however, electron excitations are expected to have sensitivity in this mass regime [9–14,17,18] (though precise results are not currently available for the SD models considered here). We consider several detector thresholds ω_{min} corresponding to capabilities of TESs expected within the next few years (40 meV) and further into the future (10 meV, 1 meV). Also shown in the plots are contours of model parameters in the magnon sensitivity region (gray).

For each benchmark DM model, magnons can probe currently unconstrained parameter space. For the vector mediator models, assuming the mediator V couples to SM particles only via kinetic mixing with the photon, V production in stellar media and in the early universe is suppressed when $m_V \to 0$, so the only astrophysical and cosmological constraints are from DM production. The latter, however, depend on whether Λ_χ is above or below the energies involved and, if below, the ultraviolet (UV) completion of the effective operators. For example, if $\Lambda_\chi \sim m_\chi$ and the UV completion involves millicharged particles [59,60] with couplings $\sim g_\chi$, we find that magnetic dipole DM with $g_\chi g_e \lesssim 10^{-10}$ satisfies all existing constraints, but can be probed by magnons. On the other hand, if $\Lambda_\chi \gtrsim \mathcal{O}(100 \text{ MeV})$, we can map the constraints derived in Ref. [61] onto the gray contours in Fig. 1, e.g., excluding $g_\chi g_e m_\chi/\Lambda_\chi \in (10^{-12}, 10^{-10}) m_\chi/m_e$ for magnetic dipole DM from SN1987A—in this case, there is a large region of unconstrained parameter space above this band (even after imposing big bang nucleosynthesis constraints) [61], which can be fully covered by our projected magnon reach. The anapole model is more challenging to discover via magnons due to the high power of momentum suppression,
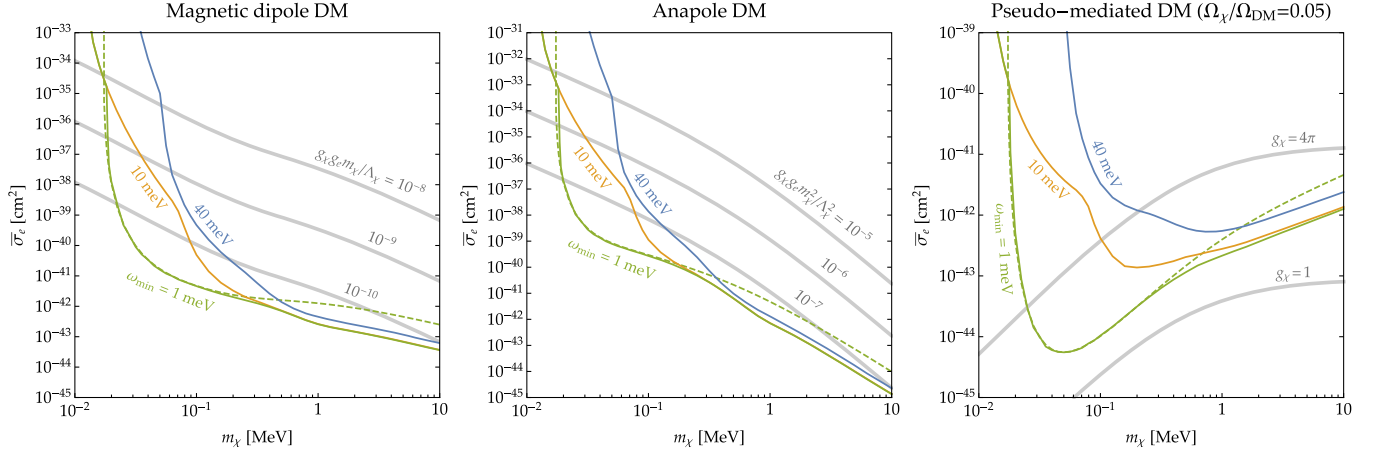
FIG. 1. Projected reach for the DM models in Table I for a YIG target, assuming three events with kilogram-year exposure, for several magnon detection thresholds ω_{min} (solid). Also shown are the results of a Heisenberg ferromagnet with the same mass and spin densities as YIG, and the same magnon dispersion as the low-energy gapless modes of YIG, for $\omega_{min} = 1$ meV (dashed); they coincide with the YIG curves for 0.02 MeV $\lesssim m_\chi \lesssim 0.1$ MeV, which can be understood from the effective theory argument in the text. The gray contours show the model parameters in the magnon sensitivity regions, which astrophysical and cosmological constraints on specified UV completions can be mapped onto (see text). For the pseudomediated model, we consider a DM subcomponent to evade SIDM constraints, and let g_e saturate the white dwarf cooling bound.

but the magnon sensitivity region still accommodates viable UV models, such as those involving two dark photons [62] which evade astrophysical and cosmological bounds altogether. Finally, for the pseudomediated DM model, the mediator-electron coupling is constrained by white dwarf cooling to be $g_e \lesssim 2 \times 10^{-13}$, so that g_χ has to be $\mathcal{O}(1)$ to produce a detectable signal. Given the existing self-interacting dark matter constraints, we consider χ to be a 5% subcomponent of DM as a viable scenario, and show contours of g_χ in Fig. 1 with g_e saturating its upper bound.

To gain some analytical intuition, we note that for momentum transfer well within the 1BZ, corresponding to $m_\chi \lesssim 0.1$ MeV for a YIG target, the rate can be estimated via an effective $n = 1$ ferromagnetic model. This is because in the $q \to 0$ limit, the external probe $\hat{\mathcal{O}}_\chi^\alpha$ acts like a uniform magnetic field. In a semiclassical picture, this causes all the spins in the target to precess in phase, so the angle between them, and thus the total energy of the Heisenberg model, stays the same. As a result, only the *gapless* mode(s), i.e., Goldstone mode(s) of the broken rotational symmetry, can be excited. Even for finite q, gapped magnon contributions are suppressed by powers of aq, where a is the lattice spacing, and thus subdominant for $q \ll a^{-1}$ ($\simeq 0.2$ keV for YIG). For a ferrimagnet like YIG, we can integrate out the gapped modes to arrive at an effective theory, where the only relevant degree of freedom is the total spin density n_s. There is only one magnon branch in this effective $n = 1$ ferromagnetic theory, which matches the gapless branch of the original ferrimagnet for $k \ll a^{-1}$. For YIG, the total spin density is $S_{cell} = (12 - 8) \times 5/2 = 10$ per unit cell volume $\Omega = a^3/2$, with $a \simeq 12.56$ Å, i.e., $n_s = 20/a^3 \simeq (4.6$ Å$)^{-3}$. The effective exchange coupling

can be shown to be $J_{eff} \simeq -4$ K $= -0.35$ meV [50], resulting in a quadratic magnon dispersion $\omega = |J_{eff}||S_{cell}|(ak)^2 \simeq k^2/(7$ MeV$)$ at small k. For this $n = 1$ ferromagnetic theory, we obtain (see the Supplemental Material [48] for details),

$$R \simeq \frac{n_s}{\rho_T} \frac{\rho_\chi}{m_\chi} \int d^3 v_\chi f(\boldsymbol{v}_\chi) \cdot$$

$$\int \frac{d^3 q}{8\pi^2} \mathrm{tr}(\hat{\rho}_\chi \hat{\mathcal{O}}_\chi^+(\boldsymbol{q}) \hat{\mathcal{O}}_\chi^{\dagger-}(\boldsymbol{q})) \delta(E_{\chi_i} - E_{\chi_f} - \omega),$$

$$\simeq 3 \ (\text{kg yr})^{-1} \left(\frac{n_s}{(4.6 \text{ Å})^{-3}}\right) \left(\frac{4.95 \text{ g/cm}^3}{\rho_T}\right) \left(\frac{0.1 \text{ MeV}}{m_\chi}\right)$$

$$\int d^3 v_\chi f(\boldsymbol{v}_\chi) \left(\frac{10^{-3}}{v_\chi}\right) \left(\frac{\hat{R}}{4 \times 10^{-27}}\right), \quad (12)$$

where $\hat{\mathcal{O}}_\chi^\pm \equiv \hat{\mathcal{O}}_\chi^1 \pm i\hat{\mathcal{O}}_\chi^2$, and

$$\hat{R} = m_e^2 \int \frac{d^3 q}{2\pi q} \mathrm{tr}(\hat{\rho}_\chi \hat{\mathcal{O}}_\chi^+ \hat{\mathcal{O}}_\chi^{\dagger-}) \delta\left(\cos\theta - \frac{q}{2m_\chi v_\chi} - \frac{\omega}{v_\chi q}\right)$$

$$= \begin{cases} \frac{2g_\chi^2 g_e^2(1+\langle c^2 \rangle)}{\Lambda_\chi^2}(q_{max}^2 - q_{min}^2) & \text{(magnetic dipole)}, \\ \frac{g_\chi^2 g_e^2(1+\langle c^2 \rangle)}{4\Lambda_\chi^4}(q_{max}^4 - q_{min}^4) & \text{(anapole)}, \\ g_\chi^2 g_e^2 \langle s^2 \rangle \log(q_{max}/q_{min}) & \text{(pseudomediated)}. \end{cases}$$

$$(13)$$

Here θ is the angle between $\boldsymbol{q}$ and $\boldsymbol{v}_\chi$, $\langle c^2 \rangle$ and $\langle s^2 \rangle$ are properly averaged values of cosine and sine squared of the angle between $\boldsymbol{q}$ and the ground state spin direction over

accessible scattering kinematics, $q_{max} \simeq 2m_\chi v_\chi$, and q_{min} is the magnon momentum for which $\omega_q = \omega_{min}$. The q dependence in Eq. (13) is indicative of dipole-dipole, quadrupole-dipole, and charge-dipole type interactions, respectively, for the three DM models.

The projected reach for this $n = 1$ Heisenberg ferromagnet is shown by the dashed curves in Fig. 1 in the $\omega_{min} = 1$ meV case, with $\langle c^2 \rangle$ set to $1/3$. We see that the full YIG results are almost exactly reproduced for $0.02 \text{ MeV} \lesssim m_\chi \lesssim 0.1 \text{ MeV}$. For $m_\chi \lesssim 0.02 \text{ MeV}$, the gapless branch becomes kinematically inaccessible, and the reach is dominated by the gapped magnons. For $m_\chi \gtrsim 0.1 \text{ MeV}$, YIG beats the $n = 1$ ferromagnet due to contributions from the gapped magnons, which are no longer suppressed as the typical momentum transfer approaches (and goes beyond) the boundaries of the 1BZ. For higher ω_{min}, effective theory predictions (not shown) are off because the lowest-energy magnon modes on the gapless branch become inaccessible.

Discussion.—While we have chosen three specific DM models for illustration, we note that there are other scenarios with SD interactions that can be probed via magnon excitation. Examples include models with a spin-1 mediator coupling to $\bar{e}\gamma^\mu\gamma^5 e$ or nonminimally to the electron. Generally, $\hat{\mathcal{O}}_\chi^\alpha$ is the mediator propagator multiplied by a function that is at least linear in q, so the rate is at least logarithmic (as in the pseudomediated model). Given the strong astrophysical and cosmological constraints on light DM and mediator scenarios [23,63,64], magnon excitations are most relevant for probing subcomponents of DM with SD interactions, if not mediated by a dark photon.

Beyond scattering, a magnon signal can also arise from absorption of bosonic DM. A prime example is an axion a interacting via $(\partial_\mu a)\bar{e}\gamma^\mu\gamma^5 e \to \nabla a \cdot \mathbf{S}_e$. However, Heisenberg-type materials with $3d$ electrons, such as YIG, have very limited sensitivity to DM absorption, because gapped modes with $k \simeq 0$, which match the kinematics, have strongly suppressed matrix elements as explained above. Here we identify three possible solutions to pursue in future work. First, in materials with nondegenerate Landé g factors (due to different orbital angular momentum admixtures in the effective spins), magnetic atoms or ions within the same unit cell can respond differently in the $q \to 0$ limit, allowing excitation of gapped magnons. Second, anisotropic spin-spin interactions can lift the otherwise gapless Goldstone modes, enabling them to match DM absorption kinematics. Finally, the gapless modes can also be lifted by an external magnetic field, which can be tuned to scan the DM mass, as considered in Refs. [52–54] (see also Ref. [65]) in the context of axion absorption.

Conclusions.—Collective excitations in condensed matter systems offer a novel detection path for light DM because of favorable kinematics. Given our ignorance of how the DM may interact with SM particles, it is important to explore different types of collective excitations in various materials in order to cover the broadest range of possibilities. In this Letter, we proposed using magnon excitations to detect DM in the 10 keV to 10 MeV mass range that couples to the electron spin. This complements previous proposals of detecting spin-independent DM interactions via phonon excitation. For a concrete demonstration of the discovery potential, we calculated the rate for three benchmark DM models, and found that currently unconstrained parameter space can be probed via magnon excitation in a YIG target.

To move forward and realize our proposed DM detection concept, a pressing question is an experimental scheme to detect magnon quanta. One possibility is calorimetric readout similar to phonon detection [30,31], in which case magnon propagation and decay, as well as magnon-TES or magnon-MKID interactions, need to be understood. Besides, recent research in quantum magnonics has taken on the challenge of resolving single magnons [66,67], and may find application in DM detection. We plan to investigate these possibilities in future work.

[1] E. D. Carlson, M. E. Machacek, and L. J. Hall, Astrophys. J. **398**, 43 (1992).

[2] C. Boehm and P. Fayet, Nucl. Phys. **B683**, 219 (2004).

[3] M. J. Strassler and K. M. Zurek, Phys. Lett. B **651**, 374 (2007).

[4] M. Pospelov, A. Ritz, and M. B. Voloshin, Phys. Lett. B **662**, 53 (2008).

[5] D. Hooper and K. M. Zurek, Phys. Rev. D **77**, 087302 (2008).

[6] J. L. Feng and J. Kumar, Phys. Rev. Lett. **101**, 231301 (2008).

[7] T. Lin, H.-B. Yu, and K. M. Zurek, Phys. Rev. D **85**, 063503 (2012).

[8] Y. Hochberg, E. Kuflik, T. Volansky, and J. G. Wacker, Phys. Rev. Lett. **113**, 171301 (2014).

[9] R. Essig, J. Mardon, and T. Volansky, Phys. Rev. D **85**, 076007 (2012).

[10] P. W. Graham, D. E. Kaplan, S. Rajendran, and M. T. Walters, Phys. Dark Universe **1**, 32 (2012).

[11] R. Essig, A. Manalaysay, J. Mardon, P. Sorensen, and T. Volansky, Phys. Rev. Lett. **109**, 021301 (2012).

[12] S. K. Lee, M. Lisanti, S. Mishra-Sharma, and B. R. Safdi, Phys. Rev. D **92**, 083517 (2015).

[13] R. Essig, M. Fernandez-Serra, J. Mardon, A. Soto, T. Volansky, and T.-T. Yu, J. High Energy Phys. 05 (2016) 046.

[14] S. Derenzo, R. Essig, A. Massari, A. Soto, and T.-T. Yu, Phys. Rev. D **96**, 016026 (2017).

[15] Y. Hochberg, T. Lin, and K. M. Zurek, Phys. Rev. D **95**, 023013 (2017).

[16] I. M. Bloch, R. Essig, K. Tobioka, T. Volansky, and T.-T. Yu, J. High Energy Phys. 06 (2017) 087.

[17] R. Essig, T. Volansky, and T.-T. Yu, Phys. Rev. D **96**, 043017 (2017).

[18] N. A. Kurinsky, T. C. Yu, Y. Hochberg, and B. Cabrera, Phys. Rev. D **99**, 123005 (2019).

[19] R. Essig, J. Mardon, O. Slone, and T. Volansky, Phys. Rev. D **95**, 056011 (2017).

[20] A. Arvanitaki, S. Dimopoulos, and K. Van Tilburg, Phys. Rev. X **8**, 041001 (2018).

[21] R. Essig, J. Pérez-Ríos, H. Ramani, and O. Slone, Phys. Rev. Research **1**, 033105 (2019).

[22] Y. Hochberg, Y. Zhao, and K. M. Zurek, Phys. Rev. Lett. **116**, 011301 (2016).

[23] Y. Hochberg, M. Pyle, Y. Zhao, and K. M. Zurek, J. High Energy Phys. 08 (2016) 057.

[24] Y. Hochberg, T. Lin, and K. M. Zurek, Phys. Rev. D **94**, 015019 (2016).

[25] Y. Hochberg, Y. Kahn, M. Lisanti, C. G. Tully, and K. M. Zurek, Phys. Lett. B **772**, 239 (2017).

[26] K. Schutz and K. M. Zurek, Phys. Rev. Lett. **117**, 121302 (2016).

[27] S. Knapen, T. Lin, and K. M. Zurek, Phys. Rev. D **95**, 056019 (2017).

[28] F. Acanfora, A. Esposito, and A. D. Polosa, Eur. Phys. J. C **79**, 549 (2019).

[29] A. Caputo, A. Esposito, and A. D. Polosa, Phys. Rev. D **100**, 116007 (2019).

[30] S. Knapen, T. Lin, M. Pyle, and K. M. Zurek, Phys. Lett. B **785**, 386 (2018).

[31] S. Griffin, S. Knapen, T. Lin, and K. M. Zurek, Phys. Rev. D **98**, 115034 (2018).

[32] S. Chang, A. Pierce, and N. Weiner, J. Cosmol. Astropart. Phys. 01 (2010) 006.

[33] A. L. Fitzpatrick and K. M. Zurek, Phys. Rev. D **82**, 075004 (2010).

[34] A. L. Fitzpatrick, W. Haxton, E. Katz, N. Lubbers, and Y. Xu, arXiv:1203.3542.

[35] M. I. Gresham and K. M. Zurek, Phys. Rev. D **89**, 123521 (2014).

[36] M. Pospelov and T. ter Veldhuis, Phys. Lett. B **480**, 181 (2000).

[37] K. Sigurdson, M. Doran, A. Kurylov, R. R. Caldwell, and M. Kamionkowski, Phys. Rev. D **70**, 083501 (2004); **73**, 089903(E) (2006).

[38] E. Masso, S. Mohanty, and S. Rao, Phys. Rev. D **80**, 036009 (2009).

[39] S. Chang, N. Weiner, and I. Yavin, Phys. Rev. D **82**, 125011 (2010).

[40] V. Barger, W.-Y. Keung, and D. Marfatia, Phys. Lett. B **696**, 74 (2011).

[41] T. Banks, J.-F. Fortin, and S. Thomas, arXiv:1007.5515.

[42] C. M. Ho and R. J. Scherrer, Phys. Lett. B **722**, 341 (2013).

[43] E. Del Nobile, G. B. Gelmini, P. Gondolo, and J.-H. Huh, J. Cosmol. Astropart. Phys. 06 (2014) 002.

[44] B. J. Kavanagh, P. Panci, and R. Ziegler, J. High Energy Phys. 04 (2019) 089.

[45] X. Chu, J. Pradler, and L. Semmelrock, Phys. Rev. D **99**, 015040 (2019).

[46] A. Auerbach, *Interacting Electrons and Quantum Magnetism* (Springer New York, New York, NY, 1994).

[47] J. M. D. Coey, *Magnetism and Magnetic Materials* (Cambridge University Press, Cambridge, England, 2001).

[48] See the Supplemental Material at http://link.aps.org/supplemental/10.1103/PhysRevLett.124.201801 for additional details of the magnon rate calculation.

[49] Magnons can also be excited via couplings to orbital angular momenta. Here we assume negligible orbital angular momenta for simplicity, noting that this is the case for many familiar materials where $3d$ electrons are responsible for the magnetic order.

[50] V. Cherepanov, I. Kolokolov, and V. L'vov, Phys. Rep. **229**, 81 (1993).

[51] A. J. Princep, R. A. Ewings, S. Ward, S. Tóth, C. Dubs, D. Prabhakaran, and A. T. Boothroyd, npj Quantum Mater. **2**, 63 (2017).

[52] R. Barbieri, M. Cerdonio, G. Fiorentini, and S. Vitale, Phys. Lett. B **226**, 357 (1989).

[53] N. Crescini *et al.*, Eur. Phys. J. C **78**, 703 (2018); **78**, 813(E) (2018).

[54] G. Flower, J. Bourhill, M. Goryachev, and M. E. Tobar, Phys. Dark Universe **25**, 100306 (2018).

[55] A. Jain, S. P. Ong, G. Hautier, W. Chen, W. D. Richards, S. Dacek, S. Cholia, D. Gunter, D. Skinner, G. Ceder, and K. A. Persson, APL Mater. **1**, 011002 (2013).

[56] S. Toth and B. Lake, arXiv:1402.6069.

[57] For calorimetric readout, the backgrounds are expected to be similar to other experiments reading out meV-eV energy depositions: radiogenic backgrounds are not expected to be problematic at such low energies, while coherent scattering from high-energy photons can be suppressed with an active veto, leaving pp solar neutrinos the main irreducible background. We expect the latter to be at most a few events per kilogram-year, as estimated from neutrino-nucleus scattering (see, e.g., Refs. [23,58]).

[58] R. Essig, M. Sholapurkar, and T.-T. Yu, Phys. Rev. D **97**, 095029 (2018).

[59] S. Davidson, S. Hannestad, and G. Raffelt, J. High Energy Phys. 05 (2000) 003.

[60] H. Vogel and J. Redondo, J. Cosmol. Astropart. Phys. 02 (2014) 029.

[61] X. Chu, J.-L. Kuo, J. Pradler, and L. Semmelrock, Phys. Rev. D **100**, 083002 (2019).

[62] E. Masso and J. Redondo, Phys. Rev. Lett. **97**, 151802 (2006).

[63] D. Green and S. Rajendran, J. High Energy Phys. 10 (2017) 013.

[64] S. Knapen, T. Lin, and K. M. Zurek, Phys. Rev. D **96**, 115021 (2017).

[65] D. J. E. Marsh, K.-C. Fong, E. W. Lentz, L. Smejkal, and M. N. Ali, Phys. Rev. Lett. **123**, 121601 (2019).

[66] D. Lachance-Quirion, Y. Tabuchi, S. Ishino, A. Noguchi, T. Ishikawa, R. Yamazaki, and Y. Nakamura, Sci. Adv. **3**, e1603150 (2017).

[67] D. Lachance-Quirion, Y. Tabuchi, A. Gloppe, K. Usami, and Y. Nakamura, Appl. Phys. Express **12**, 070101 (2019).